Technische Universität Graz

Boundary element methods for magnetostatic field problems: A critical view

Z. Andjelic, G. Of, O. Steinbach, P. Urthaler

Berichte aus dem Institut für Numerische Mathematik

Bericht 2010/5

Technische Universität Graz

Boundary element methods for magnetostatic field problems: A critical view

Z. Andjelic, G. Of, O. Steinbach, P. Urthaler

Berichte aus dem Institut für Numerische Mathematik

Bericht 2010/5

Technische Universität Graz
Institut für Numerische Mathematik
Steyrergasse 30
A 8010 Graz

WWW: `http://www.numerik.math.tu-graz.at`

Boundary element methods for magnetostatic field problems: A critical view

Z. Andjelic[1], G. Of[2], O. Steinbach[2], P. Urthaler[2]

[1]Corporate Research, ABB Switzerland Ltd.,
CH 5405 Baden–Dättwil, Switzerland

zoran.andjelic@ch.abb.com

[2]Institut für Numerische Mathematik, TU Graz,
Steyrergasse 30, A 8010 Graz, Austria

of@tugraz.at, o.steinbach@tugraz.at, urthaler@tugraz.at

Abstract

For the solution of magnetostatic field problems we discuss and compare several boundary integral formulations with respect to their accuracy, their efficiency, and their robustness. We provide fast boundary element methods which are able to deal with multiple connected computational domains, with large magnetic permeabilities, and with complicated structures with small gaps. The numerical comparison is based on several examples, including a controllable reactor as a real–world problem.

1 Introduction

An efficient and accurate numerical simulation of magnetostatic field problems contributes to the solution of challenging problems in engineering and industry. Such a simulation tool has to satisfy several requirements, for example, a robust handling of geometrical singularities at edges and corners as well as the treatment of small gaps, and the ability to handle complex real–world structures. Although not considered in this paper, an efficient treatment of nonlinearities and the coupling with other physical fields is of increasing interest. However, all approaches as described in this paper can be extended appropriately, also including a possible coupling of finite and boundary element methods.

As a model problem we consider the magnetostatic field equations where some magnetic material is placed within a bounded domain, and where a prescribed current density is applied in the surrounding unbounded air domain. For the solution of this model problem we present a comparative analysis of several boundary element based approaches emphasizing their advantages and drawbacks with respect to the above mentioned requirements. We analyze boundary integral formulations using single and double layer charge distributions, and a Steklov–Poincaré operator formulation. While all of the boundary integral equations are equivalent to each other on the continuous level, they are quite different when considering their boundary element discretizations, i.e., we compare these methods with respect to their accuracy, their efficiency, and their robustness. The aim of this paper is to highlight and, through comparison, to conclude the most suitable boundary element approach that successfully covers all of the above mentioned requirements. As a particular result of this comparison we provide accurate, efficient, and robust boundary element methods which are able to deal with multiple connected computational domains, with large magnetic permeabilities, and with complicated structures involving small gaps.

The numerical analysis of magnetostatic field problems has been widely considered in a number of references describing either finite element methods, see, e.g., [2, 5, 6, 13, 15], or boundary element methods, see, e.g., [3, 8, 10, 11, 12, 14, 16, 17, 22]. In this paper we give a unified approach for the solution of magnetostatic field problems by using a scalar magnetostatic potential and Galerkin boundary element methods for the discretization of different related boundary integral equations. Note that all boundary element formulations as discussed in this paper can be considered also within a coupling with finite element methods.

This paper is organized as follows: In Sect. 2 we describe the model problem under consideration, and we introduce a scalar magnetostatic potential to obtain a transmission problem for a Laplace equation with piecewise constant material parameters. For the solution of the resulting transmission problem we introduce three different boundary integral formulations in Sect. 3. The use of a single layer potential, which ensures the continuity of the scalar potential, results in a second kind boundary integral equation with the adjoint double layer potential. In contrast, the use of a double layer potential ensures the continuity of the fluxes, but requires a reformulation of the inhomogeneous flux transmission conditions. In this case, we have to solve a second kind boundary integral equation with the double layer potential. Based on the solution of local boundary value problems we end up with a Steklov–Poincaré operator formulation to find the unknown scalar magnetostatic potential on the interface. Finally we discuss unique solvability of all boundary integral equations, and we prove the equivalence of all formulations on the continuous level. In Sect. 4 we describe the numerical solution of all boundary integral formulations under consideration by using fast Galerkin boundary element methods. Several numerical examples are given in Sect. 5. A first example covers a sphere where we check the accuracy of the approximate solutions for an analytically known solution. As an example for a multiple connected domain we consider a ring with a square as cross section. As an example of industrial interest we consider a controllable reactor. Finally, we give some conclusions in Sect. 6.

2 Magnetostatic field problems

We consider the magnetostatic field equations for the magnetic flux density $\boldsymbol{B}$ and for the magnetic field intensity $\boldsymbol{H}$ satisfying

$$\operatorname{curl} \boldsymbol{H}(x) \;=\; \boldsymbol{j}(x), \quad \operatorname{div} \boldsymbol{B}(x) \;=\; 0, \quad \boldsymbol{B}(x) = \mu(x)\boldsymbol{H}(x) \quad \text{for } x \in \mathbb{R}^3, \tag{2.1}$$

where $\boldsymbol{j}$ is a prescribed current density. Let $\Omega \subset \mathbb{R}^3$ be some bounded domain describing some magnetic material, while in the unbounded domain $\Omega^c := \mathbb{R}^3 \backslash \overline{\Omega}$ we model air, i.e.,

$$\mu(x) = \mu_1 \quad \text{for } x \in \Omega, \quad \mu(x) = \mu_0 \quad \text{for } x \in \Omega^c, \quad 0 < \mu_0 < \mu_1 \, .$$

In addition to the above relations we include transmission conditions for $x \in \Gamma = \partial\Omega$,

$$[\boldsymbol{B}(x) \cdot n_x]_{|x\in\Gamma} \;=\; 0, \quad [\boldsymbol{H}(x) \times n_x]_{|x\in\Gamma} \;=\; 0, \tag{2.2}$$

where n_x is the exterior normal vector for $x \in \Gamma$ almost everywhere. A particular solution of Ampere's law in (2.1) is given by the Biot–Savart integral

$$\boldsymbol{H}_j(x) \;=\; \operatorname{curl}_x \int_V \frac{1}{4\pi} \frac{\boldsymbol{j}(y)}{|x-y|} dy \;=\; \frac{1}{4\pi} \int_V \boldsymbol{j}(y) \times \frac{x-y}{|x-y|^3} \, dy \quad \text{for } x \in \mathbb{R}^3, \tag{2.3}$$

where V is the support of the current $\boldsymbol{j}$ which is located somewhere in the exterior domain Ω^c. By construction we have

$$\operatorname{curl} \boldsymbol{H}_j(x) \;=\; \boldsymbol{j}(x), \quad \operatorname{div} \boldsymbol{H}_j(x) \;=\; 0 \quad \text{for } x \in \mathbb{R}^3 \tag{2.4}$$

and it remains to find the vector field $\boldsymbol{H}_0$ satisfying

$$\operatorname{curl} \boldsymbol{H}_0(x) = 0, \quad \operatorname{div} \boldsymbol{B}(x) = 0, \quad \boldsymbol{B}(x) = \mu(x)[\boldsymbol{H}_0(x) + \boldsymbol{H}_j(x)] \quad \text{for } x \in \mathbb{R}^3. \tag{2.5}$$

For this we may introduce a scalar potential

$$\boldsymbol{H}_0(x) \;=\; -\nabla\varphi(x) \quad \text{for } x \in \mathbb{R}^3 \tag{2.6}$$

to obtain the representations

$$\boldsymbol{H}(x) \;=\; \boldsymbol{H}_j(x) - \nabla\varphi(x), \quad \boldsymbol{B}(x) \;=\; \mu(x)[\boldsymbol{H}_j(x) - \nabla\varphi(x)] \quad \text{for } x \in \mathbb{R}^3 \, . \tag{2.7}$$

Therefore, by combining (2.4) and (2.5) we have to solve the potential equation

$$-\operatorname{div}[\mu(x)\nabla\varphi(x)] \;=\; 0 \quad \text{for } x \in \mathbb{R}^3 \, . \tag{2.8}$$

Instead of (2.8) we consider the local partial differential equations

$$-\Delta\varphi_1(x) = 0 \quad \text{for } x \in \Omega, \quad -\Delta\varphi_0(x) = 0 \quad \text{for } x \in \Omega^c \tag{2.9}$$

to find the local restrictions $\varphi_1 = \varphi_{|\Omega}$ and $\varphi_0 = \varphi_{|\Omega^c}$ satisfying the transmission boundary condition

$$\varphi_1(x) = \varphi_0(x) \quad \text{for } x \in \Gamma. \tag{2.10}$$

From the continuity of the normal component of the magnetic flux $\boldsymbol{B}$, see (2.2), we conclude a second transmission boundary condition, i.e.,

$$\mu_1 \frac{\partial}{\partial n_x}\varphi_1(x) - \mu_0 \frac{\partial}{\partial n_x}\varphi_0(x) \;=\; (\mu_1 - \mu_0)\, \boldsymbol{H}_j(x) \cdot n_x \quad \text{for } x \in \Gamma. \tag{2.11}$$

Finally, we have to include the radiation condition

$$\varphi_0(x) = \mathcal{O}\Big(\frac{1}{|x|}\Big) \quad \text{as } |x| \to \infty. \tag{2.12}$$

In what follows we will discuss several boundary integral formulations to solve the transmission boundary value problem (2.9)–(2.12) by using different boundary element approaches. Afterwards we will compare these different methods with respect to their accuracy, their efficiency, and their robustness.

3 Boundary integral equations

3.1 Single layer potential formulation

For the solution of the transmission boundary value problem (2.9)–(2.12) we first consider a single layer potential ansatz, i.e.,

$$\varphi(x) \;=\; \frac{1}{4\pi}\int_\Gamma \frac{1}{|x-y|} w(y) ds_y \;=:\; (\widetilde{V}w)(x) \quad \text{for } x \in \mathbb{R}^3 \backslash \Gamma, \tag{3.1}$$

where $w \in H^{-1/2}(\Gamma)$ is an unknown single layer charge. Note that by using $\varphi = \widetilde{V}w$ the local partial differential equations (2.9), the Dirichlet transmission condition (2.10), and the radiation condition (2.12) are satisfied. It remains to fulfil the Neumann transmission condition (2.11). For this we consider the interior and exterior normal derivatives

$$\frac{\partial}{\partial n_x}\varphi_{|\Omega}(x) \;=\; \frac{1}{2}w(x) + (K'w)(x), \quad \frac{\partial}{\partial n_x}\varphi_{|\Omega^c}(x) \;=\; -\frac{1}{2}w(x) + (K'w)(x) \quad \text{for } x \in \Gamma$$

which have to be understood in a weak sense. Recall, that

$$(K'w)(x) \;=\; \frac{1}{4\pi}\int_\Gamma \frac{\partial}{\partial n_x}\frac{1}{|x-y|} w(y) ds_y \quad \text{for } x \in \Gamma$$

denotes the adjoint double layer integral operator. Formally, from the Neumann transmission condition (2.11) we finally conclude the second kind boundary integral equation

$$\frac{1}{2}(\mu_1 + \mu_0) w(x) + (\mu_1 - \mu_0)(K'w)(x) \;=\; (\mu_1 - \mu_0)\, \boldsymbol{H}_j(x) \cdot n_x \quad \text{for } x \in \Gamma.$$

In particular, the single layer charge $w \in H^{-1/2}(\Gamma)$ is a solution of the boundary integral equation

$$\frac{1}{2}w(x) + \frac{\mu_1-\mu_0}{\mu_1+\mu_0}(K'w)(x) \;=\; \frac{\mu_1-\mu_0}{\mu_1+\mu_0}\boldsymbol{H}_j(x)\cdot n_x \quad \text{for } x \in \Gamma. \tag{3.2}$$

3.2 Steklov–Poincaré operator formulation

The solution of the interior Laplace equation in (2.9) is given by the representation formula

$$\varphi_1(x) = \frac{1}{4\pi}\int_\Gamma \frac{1}{|x-y|}\frac{\partial}{\partial n_y}\varphi_1(y)ds_y - \frac{1}{4\pi}\int_\Gamma \frac{\partial}{\partial n_y}\frac{1}{|x-y|}\varphi_1(y)ds_y \quad \text{for } x \in \Omega, \tag{3.3}$$

from which we obtain the boundary integral equation of the direct approach

$$\frac{1}{4\pi}\int_\Gamma \frac{1}{|x-y|}\frac{\partial}{\partial n_y}\varphi_1(y)ds_y \;=\; \frac{1}{2}\varphi_1(x) + \frac{1}{4\pi}\int_\Gamma \frac{\partial}{\partial n_y}\frac{1}{|x-y|}\varphi_1(y)ds_y \quad \text{for } x \in \Gamma. \tag{3.4}$$

By using the single and double layer integral operators

$$(Vw)(x) = \frac{1}{4\pi}\int_\Gamma \frac{1}{|x-y|}w(y)ds_y, \quad (Kv)(x) = \frac{1}{4\pi}\int_\Gamma \frac{\partial}{\partial n_y}\frac{1}{|x-y|}v(y)ds_y \quad \text{for } x \in \Gamma,$$

we can rewrite the boundary integral equation (3.4) as

$$(V\frac{\partial}{\partial n}\varphi_1)(x) \;=\; (\frac{1}{2}I + K)\varphi_1(x) \quad \text{for } x \in \Gamma.$$

Since the single layer integral operator V is invertible, we therefore obtain the Dirichlet to Neumann map

$$\frac{\partial}{\partial n_x}\varphi_1(x) \;=\; V^{-1}(\frac{1}{2}I + K)\varphi_1(x) \;=:\; (S_1\varphi_1)(x) \quad \text{for } x \in \Gamma. \tag{3.5}$$

Note that the interior Steklov–Poincaré operator S_1 admits an alternative representation, see, e.g., [24],

$$S_1 \;=\; V^{-1}(\frac{1}{2}I + K) \;=\; D + (\frac{1}{2}I + K')V^{-1}(\frac{1}{2}I + K), \tag{3.6}$$

where in addition to the adjoint double layer integral operator we used the hypersingular boundary integral operator

$$(Dv)(x) \;:=\; -\frac{1}{4\pi}\frac{\partial}{\partial n_x}\int_\Gamma \frac{\partial}{\partial n_y}\frac{1}{|x-y|}v(y)ds_y \quad \text{for } x \in \Gamma.$$

Note that the symmetric representation of the Steklov–Poincaré operator S_1 results when considering the normal derivative of the representation formula (3.3).

As in (3.3) we can describe the solution of the exterior Laplace equation in (2.9) by using the representation formula

$$\varphi_0(x) = -\frac{1}{4\pi}\int_\Gamma \frac{1}{|x-y|}\frac{\partial}{\partial n_y}\varphi_0(y)ds_y + \frac{1}{4\pi}\int_\Gamma \frac{\partial}{\partial n_y}\frac{1}{|x-y|}\varphi_0(y)ds_y \quad \text{for } x \in \Omega^c. \tag{3.7}$$

From this we conclude the boundary integral equation

$$(V\frac{\partial}{\partial n}\varphi_0)(x) \;=\; (-\frac{1}{2}I + K)\varphi_0(x) \quad \text{for } x \in \Gamma,$$

and therefore the related Dirichlet to Neumann map

$$\frac{\partial}{\partial n_x}\varphi_0(x) \;=\; -V^{-1}(\frac{1}{2}I - K)\varphi_0(x) \;=:\; -(S_0\varphi_0)(x) \quad \text{for } x \in \Gamma. \tag{3.8}$$

Again, the exterior Steklov–Poincaré operator S_0 admits an alternative representation,

$$S_0 \;=\; V^{-1}(\frac{1}{2}I - K) \;=\; D + (\frac{1}{2}I - K')V^{-1}(\frac{1}{2}I - K). \tag{3.9}$$

By using the interior and exterior Dirichlet to Neumann maps (3.5) and (3.8), respectively, and by using the Dirichlet transmission condition $\varphi(x) = \varphi_1(x) = \varphi_0(x)$ for $x \in \Gamma$, the Neumann transmission condition (2.11) can be rewritten as a boundary integral equation to find the scalar potential $\varphi \in H^{1/2}(\Gamma)$ such that

$$\mu_1(S_1\varphi)(x) + \mu_0(S_0\varphi)(x) \;=\; (\mu_1 - \mu_0)\,\boldsymbol{H}_j(x) \cdot n_x \quad \text{for } x \in \Gamma. \tag{3.10}$$

3.3 Double layer potential formulation

In (3.1) a single layer potential ansatz was used which satisfies the homogeneous Dirichlet transmission condition (2.10). Alternatively one may use a double layer potential to describe the solutions of the local partial differential equations (2.9). But due to the jump relations, the interior and exterior normal derivatives of the double layer potential are continuous, but the interior and exterior Dirichlet traces are discontinuous. Hence we will reformulate the transmission problem (2.9)–(2.12) in an appropriate way to be able to use a double layer potential ansatz.

First, we define φ_j as a solution of the interior Neumann boundary value problem

$$-\Delta\varphi_j(x) \;=\; 0 \quad \text{for } x \in \Omega, \qquad \frac{\partial}{\partial n_x}\varphi_j(x) = \boldsymbol{H}_j(x) \cdot n_x \quad \text{for } x \in \Gamma. \tag{3.11}$$

To ensure solvability of this boundary value problem, we need to assume the solvability condition

$$\int_\Gamma \boldsymbol{H}_j(x) \cdot n_x\, ds_x = \int_\Omega \operatorname{div} \boldsymbol{H}_j(x)\, dx \;=\; 0,$$

which is satisfied for any bounded domain with only one surface, i.e., we may also consider multiple connected domains Ω such as a torus. We will use the first boundary integral equation to determine φ_j from

$$(\frac{1}{2}I + K)\varphi_j(x) = V(\boldsymbol{H}_j \cdot n)(x). \tag{3.12}$$

Additionally, we enforce the constraint $\int_\Gamma \varphi_j(x) ds_x = 0$ to get a unique φ_j, see, e.g., [24].

Remark 3.1 *For simply connected domains* Ω *the potential* φ_j *can be computed by using path integrals* [11, 22]. *In contrast, the presented approach is applicable to both simply and multiple connected domains. In the case of simply connected domains the gradient of* φ_j *equals* $\boldsymbol{H}_j$*, see Lemma* 3.4.

For the solution of the transmission problem (2.9)–(2.12) we now consider the ansatz

$$\varphi_1(x) := \frac{1}{\mu_1}[\widetilde{\varphi}_1(x) + (\mu_1 - \mu_0)\varphi_j(x)] \quad \text{for } x \in \Omega, \quad \varphi_0(x) := \frac{1}{\mu_0}\widetilde{\varphi}_0(x) \quad \text{for } x \in \Omega^c, \tag{3.13}$$

where $\widetilde{\varphi}_1$ and $\widetilde{\varphi}_0$ are solutions of the local partial differential equations

$$-\Delta\widetilde{\varphi}_1(x) = 0 \quad \text{for } x \in \Omega, \quad -\Delta\widetilde{\varphi}_0(x) = 0 \quad \text{for } x \in \Omega^c. \tag{3.14}$$

From the Neumann transmission condition (2.11) we then conclude

$$\begin{aligned}
\mu_1 \frac{\partial}{\partial n_x}\varphi_1(x) - \mu_0 \frac{\partial}{\partial n_x}\varphi_0(x) &= \frac{\partial}{\partial n_x}\widetilde{\varphi}_1(x) + (\mu_1 - \mu_0)\frac{\partial}{\partial n_x}\varphi_j(x) - \frac{\partial}{\partial n_x}\widetilde{\varphi}_0(x) \\
&= \frac{\partial}{\partial n_x}\widetilde{\varphi}_1(x) - \frac{\partial}{\partial n_x}\widetilde{\varphi}_0(x) + (\mu_1 - \mu_0)\boldsymbol{H}_j(x) \cdot n_x,
\end{aligned}$$

i.e., we have to require the homogeneous Neumann transmission conditions

$$\frac{\partial}{\partial n_x}\widetilde{\varphi}_1(x) - \frac{\partial}{\partial n_x}\widetilde{\varphi}_0(x) = 0 \quad \text{for } x \in \Gamma. \tag{3.15}$$

For the Dirichlet transmission condition (2.10) we obtain

$$\frac{1}{\mu_1}[\widetilde{\varphi}_1(x) + (\mu_1 - \mu_0)\varphi_j(x)] = \frac{1}{\mu_0}\widetilde{\varphi}_0(x) \quad \text{for } x \in \Gamma,$$

i.e., we conclude the inhomogeneous Dirichlet transmission conditions

$$\mu_0\widetilde{\varphi}_1(x) + (\mu_1 - \mu_0)\mu_0\varphi_j(x) = \mu_1\widetilde{\varphi}_0(x) \quad \text{for } x \in \Gamma. \tag{3.16}$$

Finally, instead of the radiation condition (2.12) we now have to require

$$\widetilde{\varphi}_0(x) = \mathcal{O}\Big(\frac{1}{|x|}\Big) \quad \text{as } |x| \to \infty\,. \tag{3.17}$$

Instead of the original transmission problem (2.9)–(2.12) we now solve the equivalent transmission problem (3.14)–(3.17). For this we may consider the double layer potential ansatz

$$\widetilde{\varphi}(x) = -(Wv)(x) = -\int_\Gamma \frac{\partial}{\partial n_y}U^*(x,y)v(y)ds_y \quad \text{for } x \in \mathbb{R}^3\backslash\Gamma, \tag{3.18}$$

where $v \in H^{1/2}(\Gamma)$ is an unknown double layer charge. By using the restrictions $\widetilde{\varphi}_1 = \widetilde{\varphi}_{|\Omega}$ and $\widetilde{\varphi}_0 = \widetilde{\varphi}_{|\Omega^c}$, the local partial differential equations (3.14), the Neumann transmission condition (3.15), and the radiation condition (3.17) are satisfied. It remains to fulfil the Dirichlet transmission condition (3.16). The application of the interior and exterior trace operators to the double layer potential (3.18) gives

$$\mu_1(\frac{1}{2}I + K)v(x) + \mu_0(\frac{1}{2}I - K)v(x) + (\mu_1 - \mu_0)\mu_0\varphi_j(x) \;=\; 0 \quad \text{for } x \in \Gamma.$$

In particular, the double layer charge $v \in H^{1/2}(\Gamma)$ is a solution of the boundary integral equation

$$\frac{1}{2}v(x) + \frac{\mu_1 - \mu_0}{\mu_1 + \mu_0}(Kv)(x) \;=\; -\frac{\mu_1 - \mu_0}{\mu_1 + \mu_0}\mu_0\varphi_j(x) \quad \text{for } x \in \Gamma. \tag{3.19}$$

3.4 Unique solvability of boundary integral equations

In the previous subsections we have presented three different boundary integral formulations to describe the solution of the transmission problem (2.9)–(2.12), and therefore of the magnetostatic field equations (2.1). It turns out that, on the continuous level, all formulations are equivalent to each other.

Theorem 3.1 *Let $w \in H^{-1/2}(\Gamma)$ be a solution of the single layer integral operator equation* (3.2)*, let $\varphi \in H^{1/2}(\Gamma)$ be a solution of the Steklov–Poincaré operator equation* (3.10)*, and let $v \in H^{1/2}(\Gamma)$ be a solution of the double layer integral operator equation* (3.19)*. Then there hold the following relations*

$$\varphi(x) \;=\; (Vw)(x) \;=\; -\frac{1}{\mu_0}(\frac{1}{2}I + K)v(x) \quad \textit{for all } x \in \Gamma.$$

Proof. Let us first rewrite the single layer potential boundary integral equation (3.2) as

$$\mu_1(\frac{1}{2}I + K')w(x) + \mu_0(\frac{1}{2}I - K')w(x) \;=\; (\mu_1 - \mu_0)\boldsymbol{H}_j(x) \cdot n_x \quad \text{for } x \in \Gamma,$$

and in the following, by using the identity $I = V^{-1}V$, as

$$\mu_1(\frac{1}{2}I + K')V^{-1}Vw(x) + \mu_0(\frac{1}{2}I - K')V^{-1}Vw(x) \;=\; (\mu_1 - \mu_0)\boldsymbol{H}_j(x) \cdot n_x \quad \text{for } x \in \Gamma.$$

With the symmetry relation $VK' = KV$, see, e.g., [24], we conclude $K'V^{-1} = V^{-1}K$ and therefore we obtain

$$\mu_1 V^{-1}(\frac{1}{2}I + K)Vw(x) + \mu_0 V^{-1}(\frac{1}{2}I - K)Vw(x) \;=\; (\mu_1 - \mu_0)\boldsymbol{H}_j(x) \cdot n_x \quad \text{for } x \in \Gamma.$$

With the Steklov–Poincaré operators $S_1 = V^{-1}(\frac{1}{2}I + K)$ and $S_0 = V^{-1}(\frac{1}{2}I - K)$ we further obtain

$$\mu_1 S_1 Vw(x) + \mu_0 V^{-1} S_0 Vw(x) \;=\; (\mu_1 - \mu_0)\boldsymbol{H}_j(x) \cdot n_x \quad \text{for } x \in \Gamma,$$

which shows the equivalence with the Steklov–Poincaré operator equation (3.10) when introducing $\varphi = Vw$.

Let us now consider the double layer integral operator equation (3.19), i.e.,

$$\mu_1(\frac{1}{2}I + K)v(x) + \mu_0(\frac{1}{2}I - K)v(x) + (\mu_1 - \mu_0)\mu_0\varphi_j(x) \; = \; 0 \quad \text{for } x \in \Gamma.$$

Recall, that φ_j is a solution of the Neumann boundary value problem (3.11). Hence, by using the boundary integral equation

$$(\frac{1}{2}I + K)\varphi_j(x) = (V[\boldsymbol{H}_j \cdot n])(x) \quad \text{for } x \in \Gamma,$$

and by multiplying the double layer integral operator equation with $(\frac{1}{2}I + K)$ we obtain

$$\mu_1(\frac{1}{2}I + K)(\frac{1}{2}I + K)v(x) + \mu_0(\frac{1}{2}I + K)(\frac{1}{2}I - K)v(x) + (\mu_1 - \mu_0)\mu_0(\frac{1}{2}I + K)\varphi_j(x) \; = \; 0,$$

and therefore

$$\mu_1(\frac{1}{2}I + K)(\frac{1}{2}I + K)v(x) + \mu_0(\frac{1}{2}I + K)(\frac{1}{2}I - K)v(x) + (\mu_1 - \mu_0)\mu_0(V[\boldsymbol{H}_j \cdot n])(x) \; = \; 0.$$

Recall that

$$\mu_0\varphi(x) = \widetilde{\varphi}_0(x) = -(\frac{1}{2}I + K)v(x) \quad \text{for } x \in \Gamma.$$

Hence we conclude

$$\mu_1(\frac{1}{2}I + K)[-\mu_0\varphi(x)] + \mu_0(\frac{1}{2}I - K)[-\mu_0\varphi(x)] + (\mu_1 - \mu_0)\mu_0(V[\boldsymbol{H}_j \cdot n])(x) \; = \; 0,$$

and in the following

$$\mu_1(\frac{1}{2}I + K)\varphi(x) + \mu_0(\frac{1}{2}I - K)\varphi(x) - (\mu_1 - \mu_0)(V[\boldsymbol{H}_j \cdot n])(x) \; = \; 0.$$

An application of the inverse single layer integral operator V^{-1} finally results in the Steklov–Poincaré operator equation (3.10). ■

Remark 3.2 *Note that the single layer potential formulation* (3.2) *as well as the double layer potential formulation* (3.19)*, which seem to be indirect approaches, can be rewritten as direct formulations, see, e.g.,* [14].

As a corollary of Theorem 3.1 we conclude, that unique solvability of one boundary integral formulation implies unique solvability of the remaining ones. Let us first consider the second kind boundary integral equation (3.19), or equivalently, the second kind boundary integral equation (3.2).

Theorem 3.2 *Let $0 < \mu_0 \leq \mu_1$. The operator*

$$\frac{1}{2}I + \frac{\mu_1 - \mu_0}{\mu_1 + \mu_0}K \;=\; I - \left(\frac{1}{2}I - \frac{\mu_1 - \mu_0}{\mu_1 + \mu_0}K\right) \;:\; H^{1/2}(\Gamma) \to H^{1/2}(\Gamma)$$

admits a unique inverse by the Neumann series

$$\left(\frac{1}{2}I + \frac{\mu_1 - \mu_0}{\mu_1 + \mu_0}K\right)^{-1} \;=\; \sum_{k=0}^{\infty} \left(\frac{1}{2}I - \frac{\mu_1 - \mu_0}{\mu_1 + \mu_0}K\right)^{k},$$

i.e., the operator

$$\frac{1}{2}I - \frac{\mu_1 - \mu_0}{\mu_1 + \mu_0}K \;:\; H^{1/2}(\Gamma) \to H^{1/2}(\Gamma)$$

is a contraction satisfying

$$\| \left(\frac{1}{2}I - \frac{\mu_1 - \mu_0}{\mu_1 + \mu_0}K\right) v\|_{V^{-1}} \;\leq\; \frac{1}{2}\left(1 + \frac{\mu_1 - \mu_0}{\mu_1 + \mu_0}\right) \|v\|_{V^{-1}} \quad \textit{for all } v \in H^{1/2}(\Gamma).$$

Proof. For $v \in H^{1/2}(\Gamma)$ we use an equivalent norm which is induced by the inverse single layer boundary integral operator,

$$\|v\|_{V^{-1}} \;:=\; \sqrt{\langle V^{-1}v, v\rangle_\Gamma}\,.$$

Note that we have, see, e.g., [26],

$$\|(\frac{1}{2}I - K)v\|_{V^{-1}} \leq \|v\|_{V^{-1}} \quad \text{for all } v \in H^{1/2}(\Gamma),$$

where the equality holds for all constant v. Then,

$$\begin{aligned}
\| \left(\frac{1}{2}I - \frac{\mu_1 - \mu_0}{\mu_1 + \mu_0}K\right) v\|_{V^{-1}} \;&=\; \|\frac{\mu_1 - \mu_0}{\mu_1 + \mu_0}(\frac{1}{2}I - K)v + \frac{1}{2}\left(1 - \frac{\mu_1 - \mu_0}{\mu_1 + \mu_0}\right) v\|_{V^{-1}} \\
&\leq\; \frac{\mu_1 - \mu_0}{\mu_1 + \mu_0}\|(\frac{1}{2}I - K)v\|_{V^{-1}} + \frac{1}{2}\left(1 - \frac{\mu_1 - \mu_0}{\mu_1 + \mu_0}\right) \|v\|_{V^{-1}} \\
&\leq\; \left[\frac{\mu_1 - \mu_0}{\mu_1 + \mu_0} + \frac{1}{2}\left(1 - \frac{\mu_1 - \mu_0}{\mu_1 + \mu_0}\right)\right] \|v\|_{V^{-1}} \\
&=\; \frac{1}{2}\left(1 + \frac{\mu_1 - \mu_0}{\mu_1 + \mu_0}\right) \|v\|_{V^{-1}}.
\end{aligned}$$

■

As a corollary of Theorem 3.2 we conclude the unique solvability of the double layer boundary integral operator equation (3.19) in $H^{1/2}(\Gamma)$, and of the single layer boundary integral operator equation (3.2) in $H^{-1/2}(\Gamma)$. Note that the contraction rate as given in Theorem 3.2 degenerates as $\mu_1 \to \infty$.

To investigate the unique solvability of the Steklov–Poincaré operator equation (3.10) we can use an ellipticity estimate as follows.

Theorem 3.3 *The boundary integral operator*

$$\mu_1 S_1 + \mu_0 S_0 : H^{1/2}(\Gamma) \to H^{-1/2}(\Gamma)$$

is $H^{1/2}(\Gamma)$–elliptic satisfying

$$\langle (\mu_1 S_1 + \mu_0 S_0) v, v\rangle_\Gamma \geq \mu_0 \langle S_0 v, v\rangle_\Gamma \geq \mu_0 (1 - c_K) \|v\|^2_{V^{-1}} \quad \textit{for all } v \in H^{1/2}(\Gamma),$$

where $c_K < 1$ is the contraction rate of $\frac{1}{2}I + K$.

Proof. The Steklov–Poincaré operator S_1, which is related to the interior Dirichlet boundary value problem, is only positive semi–definite, i.e.,

$$\langle S_1 v, v\rangle_\Gamma \geq 0 \quad \text{for all } v \in H^{1/2}(\Gamma),$$

where equality holds for all constant functions v. Moreover, the Steklov–Poincaré operator S_0 is $H^{1/2}(\Gamma)$–elliptic satisfying

$$\begin{aligned} \langle S_0 v, v\rangle_\Gamma &= \langle V^{-1}(\frac{1}{2}I - K)v, v\rangle_\Gamma \;=\; \langle V^{-1}v, v\rangle_\Gamma - \langle V^{-1}(\frac{1}{2}I + K)v, v\rangle_\Gamma \\ &\geq \langle V^{-1}v, v\rangle_\Gamma - \|(\frac{1}{2}I + K)v\|_{V^{-1}} \|v\|_{V^{-1}} \;\geq\; (1 - c_K)\|v\|^2_{V^{-1}}. \end{aligned}$$

From this we obtain the assertion. ■

For an application of a boundary element method, instead of the Steklov–Poincaré operator equation (3.10) we will consider a system of boundary integral equations, which is based on the use of the symmetric representations as given in (3.6) and (3.9), respectively. In this case we can rewrite (3.10) as

$$\begin{aligned} \mu_1 [D + (\frac{1}{2}I + K')V^{-1}(\frac{1}{2}I + K)]\varphi(x) + \mu_0 [D + (\frac{1}{2}I - K')V^{-1}(\frac{1}{2}I - K)]\varphi(x) \\ = (\mu_1 - \mu_0)\boldsymbol{H}_j(x) \cdot n_x \quad \text{for } x \in \Gamma\,. \end{aligned}$$

By introducing

$$t_1 = \mu_1 V^{-1}(\frac{1}{2}I + K)\varphi \in H^{-1/2}(\Gamma), \quad t_0 = \mu_0 V^{-1}(\frac{1}{2}I - K)\varphi \in H^{-1/2}(\Gamma)$$

we obtain a system of boundary integral equations,

$$\begin{aligned} (\mu_1 + \mu_0) D\varphi + (\frac{1}{2}I + K')t_1(x) + (\frac{1}{2}I - K')t_0(x) &= (\mu_1 - \mu_0)\boldsymbol{H}_j(x) \cdot n_x \quad \text{for } x \in \Gamma, \\ \frac{1}{\mu_1}(Vt_1)(x) - (\frac{1}{2}I + K)\varphi(x) &= 0 \quad \text{for } x \in \Gamma, \\ \frac{1}{\mu_0}(Vt_0)(x) - (\frac{1}{2}I - K)\varphi(x) &= 0 \quad \text{for } x \in \Gamma. \end{aligned}$$

Unique solvability of the above system follows from the unique solvability of the Steklov–Poincaré operator equation (3.10). Moreover, we can prove an ellipticity estimate for the bilinear form which is related to the above system of boundary integral equations.

3.5 Evaluation of the magnetic field

After determining the scalar potential φ as the solution of the transmission problem (2.9)–(2.12) we may use the representation (2.7) to compute the magnetic field

$$\boldsymbol{H}(x) \;=\; \boldsymbol{H}_j(x) - \nabla\varphi(x) \quad \text{for } x \in \mathbb{R}^3.$$

It is well known that, if Ω is simply connected,

$$\boldsymbol{H}(x) \;=\; \boldsymbol{H}_j(x) - \nabla\varphi_1(x) \;\to\; 0 \quad \text{for } x \in \Omega \quad \text{as } \mu_1 \to \infty.$$

In particular for large μ_1 there holds

$$\nabla\varphi_1(x) \approx \boldsymbol{H}_j(x) \quad \text{for } x \in \Omega.$$

For small relative errors of the numerical approximation of $\nabla\varphi_1$ we observe large relative errors for the approximation of $\boldsymbol{H}$. Therefore we are interested in an alternative approach to compute the magnetic field in Ω more robustly. For this we consider the approach as described in Subsect. 3.3, where the scalar potential was given by

$$\varphi_1(x) = \frac{1}{\mu_1}[\widetilde{\varphi}_1(x) + (\mu_1 - \mu_0)\varphi_j(x)] \quad \text{for } x \in \Omega,$$

and where φ_j is a solution of the Neumann boundary value problem (3.11). From (2.7) we then obtain

$$\begin{aligned}
\boldsymbol{B}(x) &= \mu_1[\boldsymbol{H}_j(x) - \nabla\varphi_1(x)] \\
&= \mu_0\boldsymbol{H}_j(x) - \nabla\widetilde{\varphi}_1(x) + (\mu_1 - \mu_0)[\boldsymbol{H}_j(x) - \nabla\varphi_j(x)] \\
&= \mu_0\boldsymbol{H}_j(x) - \nabla\widetilde{\varphi}_1(x) \quad \text{for } x \in \Omega,
\end{aligned} \tag{3.20}$$

where we used the following result.

Lemma 3.4 *Let φ_j be a solution of the Neumann boundary value problem* (3.11), *i.e.,*

$$-\Delta\varphi_j(x) = 0 \quad \textit{for } x \in \Omega, \qquad \frac{\partial}{\partial n_x}\varphi_j(x) = \boldsymbol{H}_j(x)\cdot n_x \quad \textit{for } x \in \Gamma,$$

where $\boldsymbol{H}_j(x)$ is given as in (2.3). *Additionally, let a simply connected domain $\Omega_s \supset \Omega$ exist such that $\operatorname{supp} j \cap \Omega_s = \emptyset$. Then there holds $\boldsymbol{H}_j(x) = \nabla\varphi_j(x)$ for almost all $x \in \Omega$.*

Proof. From Green's first formula and by using the Neumann boundary condition we have for all $\psi \in H^1(\Omega)$

$$\int_\Omega \nabla\varphi_j(x)\cdot\nabla\psi(x)dx \;=\; \int_\Gamma \frac{\partial}{\partial n_x}\varphi_j(x)\psi(x)ds_x \;=\; \int_\Gamma [\boldsymbol{H}_j(x)\cdot n_x]\psi(x)ds_x.$$

On the other hand, by using integration by parts and (2.4), we get

$$\begin{aligned}\int_\Gamma [\boldsymbol{H}_j(x)\cdot n_x]\psi(x)ds_x &= \int_\Omega [\operatorname{div}\boldsymbol{H}_j(x)\,\psi(x)+\boldsymbol{H}_j(x)\cdot\nabla\psi(x)]\;dx\\ &= \int_\Omega \boldsymbol{H}_j(x)\cdot\nabla\psi(x)\,dx,\end{aligned}$$

and therefore

$$\int_\Omega [\boldsymbol{H}_j(x)-\nabla\varphi(x)]\cdot\nabla\psi(x)dx \quad \text{for all } \psi\in H^1(\Omega)$$

follows. Since Ω_s is simply connected and $\operatorname{curl}\boldsymbol{H}_j(x)=0$ for $x\in\Omega_s$, $\boldsymbol{H}_j$ can be written as a gradient field in Ω_s. Insertion of $\psi=\boldsymbol{H}_j-\nabla\varphi$ concludes the identity in the sense of $L_2(\Omega)$. ■

Remark 3.3 *Lemma* 3.4 *can be used for the evaluation of the excitation field inside a simply connected domain* Ω*.*

i. For the single layer potential ansatz as described in Subsect. 3.1 *the excitation field* $\boldsymbol{H}_j$ *is represented by solving*

$$\frac{1}{2}w_j(x)+(K'w_j)(x) \;=\; \boldsymbol{H}_j(x)\cdot n_x \quad \textit{for}\, x\in\Gamma$$

and finally the evaluation reads

$$\boldsymbol{H}(x)=(\nabla\widetilde{V}w_j)(x)-(\nabla\widetilde{V}w)(x) \quad \textit{for}\, x\in\Omega.$$

ii. For the Steklov–Poincaré operator formulation as used in Subsect. 3.2 *the equation*

$$(S_1\varphi_j)(x) \;=\; \boldsymbol{H}_j(x)\cdot n_x \quad \textit{for}\, x\in\Gamma \tag{3.21}$$

is solved and the associated Neumann datum is calculated by

$$\frac{\partial}{\partial n_x}\varphi_j(x)=(S_1\varphi_j)(x) \quad \textit{for}\, x\in\Gamma.$$

Finally the excitation field can be evaluated as the gradient of a representation formula for $\varphi_j(x)$*,* $x\in\Omega$*.*

The projection of $\boldsymbol{H}_j$ *to the same spaces as* $\boldsymbol{H}_0$ *provides a more accurate evaluation of* $\boldsymbol{H}(x)$*,* $x\in\Omega$*, for the discrete approximation of these two approaches* [12].

4 Boundary element methods

We describe briefly the discrete systems of linear equations and the approximate computation of $\boldsymbol{H}$. For details on boundary element methods see, e.g., [21]. For all presented approaches, we use a Galerkin variational formulation to solve the boundary integral equations.

4.1 Single layer potential formulation

The Galerkin variational formulation of the boundary integral equation (3.2) is to find a piecewise constant approximation $w_h \in S_h^0(\Gamma) = \mathrm{span}\{\psi_\ell^0\}_{\ell=1}^N$ such that

$$\langle (\frac{\mu_1+\mu_0}{\mu_1-\mu_0}\frac{1}{2}I + K')w_h, z_h\rangle_\Gamma = \langle \boldsymbol{H}_j \cdot n, z_h\rangle_\Gamma$$

is satisfied for all $z_h \in S_h^0(\Gamma)$. This is equivalent to a linear system of algebraic equations,

$$\left(\frac{1}{2}\frac{\mu_1+\mu_0}{\mu_1-\mu_0}\widetilde{M}_h + \widetilde{K}_h'\right)\underline{w} = \underline{f}^0$$

where for $k, \ell = 1, \ldots, N$

$$\widetilde{M}_h[k,\ell] = \langle \psi_\ell^0, \psi_k^0\rangle_\Gamma, \quad \widetilde{K}_h'[k,\ell] = \langle K'\psi_\ell^0, \psi_k^0\rangle_\Gamma, \quad f_k^0 = \langle \boldsymbol{H}_j \cdot n, \psi_k^0\rangle_\Gamma.$$

In the case of a simply connected domain Ω, we use an indirect single layer approach to solve the interior boundary value (3.11),

$$\frac{1}{2}w_j(x) + (K'w_j)(x) = \boldsymbol{H}_j(x)\cdot n_x \quad \text{for } x \in \Gamma, \quad \int_\Gamma w_j(x)ds_x = 0. \tag{4.1}$$

Thus we compute, in the case of a simply connected domain, an approximation $w_{j,h} \in S_h^0(\Gamma)$ of the density function w_j in (4.1) as the solution of

$$\left(\frac{1}{2}\widetilde{M}_h + \widetilde{K}_h' + \underline{a}\,\underline{a}^\top\right)\underline{w}_j = \underline{f}^0 \tag{4.2}$$

where for $k = 1, \ldots, N$

$$a_k = \langle \psi_k^0, 1\rangle_\Gamma.$$

We utilize the rank one term $\underline{a}\,\underline{a}^\top$ to get a uniquely solvable system of linear equations and to fix the constant part of the non–unique solution of the Neumann boundary value problem (3.11). The linear systems are solved by a GMRES method with a simple diagonal preconditioning. To compute $\boldsymbol{H}$ we evaluate

$$\boldsymbol{H}(x) = \nabla\widetilde{V}(w_{j,h} - w_h)(x) \quad \text{for } x \in \Omega$$

in the case of a simply connected domain Ω and otherwise

$$\boldsymbol{H}(x) = \boldsymbol{H}_j(x) - \nabla(\widetilde{V}w_h)(x) \quad \text{for } x \in \mathbb{R}^3.$$

4.2 Double layer potential formulation

Here, we approximate the unknown density v by $v_h \in S_h^1(\Gamma) = \text{span}\{\psi_m^1\}_{m=1}^M$ by using piecewise linear and continuous basis functions ψ_m^1 which are defined with respect to an admissible triangulation of the boundary. First, we determine an approximation of the interior Neumann boundary value problem (3.11) based on the boundary integral equation (3.12) by the system of linear equations

$$(\frac{1}{2}\widehat{M}_h + \widehat{K}_h + \underline{b}\,\underline{b}^\top)\underline{\varphi}_j = \widehat{V}_h \underline{g}$$

where for $m, n = 1, \ldots, M$, $\ell = 1, \ldots, N$

$$\widehat{M}_h[m,n] = \langle \psi_n^1, m_k^1 \rangle_\Gamma,\ \widehat{K}_h[m,n] = \langle K\psi_n^1, \psi_m^1 \rangle_\Gamma,\ \widehat{V}_h[m,\ell] = \langle V\psi_\ell^0, \psi_m^1 \rangle_\Gamma,\ b_m = \langle \psi_m^1, 1 \rangle_\Gamma,$$

and $\underline{g} \in \mathbb{R}^M$ is the vector of the L_2 projection $g_h \in S_h^0(\Gamma)$ of $\boldsymbol{H}_j \cdot n$ onto the space of piecewise constant functions. As before, the linear system is solved by a GMRES method with diagonal preconditioning.

Remark 4.1 *If we apply the indirect ansatz* (4.1) *to solve the interior boundary value problem* (3.11)*, we end up with a worse approximation of the magnetic field, see the example considered in* [18]*. In general, density functions of indirect approaches show a lower regularity than the direct quantities, see, e.g.,* [4, 20]*. In this case, the approximation order of the discrete approximation is reduced.*

The Galerkin discretization of the boundary integral equation (3.19) by using piecewise linear and continuous basis functions ψ_m^1, i.e. we have $v_h \in S_h^1(\Gamma)$, results in the linear system of algebraic equations

$$\left(\frac{1}{2}\frac{\mu_1 + \mu_0}{\mu_1 - \mu_0}\widehat{M}_h + \widehat{K}_h\right)\underline{v} = \widehat{M}_h \underline{\varphi}_j$$

which is again solved by a GMRES method with diagonal preconditioning.

Based on the ansatz (3.13) we evaluate $\boldsymbol{H}$ by

$$\boldsymbol{H}(x) = \boldsymbol{H}_j(x) + \frac{1}{\mu_0}\nabla(Wv_h)(x) \quad \text{for } x \in \Omega^c$$

and

$$\boldsymbol{H}(x) = \boldsymbol{H}_j(x) + \frac{1}{\mu_1}\nabla(Wv_h)(x) - \frac{\mu_1 - \mu_0}{\mu_1}\Big((\widetilde{V}\varphi_{j,h})(x) - (Wg_h)(x)\Big) \quad \text{for } x \in \Omega,$$

and in the case of a simply connected domain by using (3.20)

$$\boldsymbol{H}(x) = \frac{\mu_0}{\mu_1}\boldsymbol{H}_j(x) + \frac{1}{\mu_1}\nabla(Wv_h)(x) \quad \text{for } x \in \Omega.$$

4.3 Steklov–Poincaré operator formulation

For the Galerkin discretization of the Steklov–Poincaré operator equation (3.10) we use piecewise linear and continuous basis function ψ_m^1, i.e., we have $\varphi_h \in S_h^1(\Gamma)$. In this case we have to solve the linear system of algebraic equations

$$(\mu_1 S_{1,h} + \mu_0 S_{0,h})\,\underline{\varphi} = (\mu_1 - \mu_0)\underline{f}^1, \tag{4.3}$$

where for $k = 1, \dots, M$

$$f_k^1 = \langle \boldsymbol{H}_j \cdot n, \psi_k^1 \rangle_\Gamma.$$

Since a direct discretization of the Steklov–Poincaré operators S_0 and S_1 is not possible in general, we use the approximations

$$S_{1,h} = D_h + (\frac{1}{2}M_h^\top + K_h^\top)V_h^{-1}(\frac{1}{2}M_h + K_h), \quad S_{0,h} = D_h + (\frac{1}{2}M_h^\top - K_h^\top)V_h^{-1}(\frac{1}{2}M_h - K_h)$$

where

$$D_h[m,n] = \langle D\psi_n^1, \psi_m^1 \rangle_\Gamma, K_h[k,n] = \langle K\psi_n^1, \psi_k^0 \rangle_\Gamma, M_h[k,n] = \langle \psi_n^1, \psi_k^0 \rangle_\Gamma, V_h[k,\ell] = \langle V\psi_\ell^0, \psi_k^0 \rangle_\Gamma$$

for $m, n = 1, \dots, M$ and $k, \ell = 1, \dots, N$. We use an artificial multilevel preconditioner [23] for the preconditioning of the iterative inversion of V_h by a CG method, and the application of an operator of opposite order [25] for the iterative solution of the global system (4.3) again by a CG method. Finally we solve

$$V_h \underline{t}_1 = (\frac{1}{2}M_h + K_h)\underline{\varphi}, \quad V_h \underline{t}_0 = (\frac{1}{2}M_h - K_h)\underline{\varphi}$$

to obtain the complete Cauchy data. Then the magnetic field is evaluated based on the representation formulae (3.3) and (3.7), respectively. On the transmission interface we can build the linear combination

$$\boldsymbol{H}(x_k) = \boldsymbol{H}_j(x_k) - (t_{i,k} n_k + \nabla_t \varphi_h(x_k))$$

with the tangential derivative ∇_t to evaluate the magnetic field in the centers x_k of the triangles τ_k with normal direction n_k. In the case of a simply connected domain we replace $\boldsymbol{H}_j$ in the evaluation as described in Remark 3.3.

We use the fast multipole method [9] for a data–sparse discretization and for a fast application of all boundary integral operators of the systems of linear equations and for the evaluation of the magnetic field. For details, see [19] and the references therein.

5 Numerical results

In this section, we present several examples to compare the accuracy of the approximate solutions of the presented approaches to solve the transmission problem (2.9)–(2.12). In addition, we comment on the advantages and the drawbacks of the discussed approaches and present some computational times. In all examples, we consider $\mu_0 = 4\pi \cdot 10^{-7}$ and $\mu_1 = \mu_0 \mu_r$ with different values of the relative permeability μ_r.

5.1 Sphere

We first consider a sphere of diameter 10^{-3} to check the accuracy of the approximate solutions for an analytically known solution. For a given excitation field $\boldsymbol{H}_c = (0,0,17)^\top$ the resulting magnetic field is given by $\boldsymbol{H} = (0,0,51/(\mu_r+2))^\top$, see [12]. In Figure 1, the relative $L_2(\Gamma)$ errors of the approximate solutions of $\boldsymbol{H}$ are given for several values of μ_r and for an approximation of the sphere by 288 plane triangles. The single layer potential formulation (SL) is compared to the direct Steklov–Poincaré operator formulation (SP) and the double layer potential formulation (DL). Since the sphere is simply connected, approximation problems appear for higher μ_r. This problem has been discussed in Subsection 3.5, which concluded in the modified evaluation as discussed in Remark 3.3 for the single layer potential ansatz and the Steklov–Poincaré operator formulation and in formula (3.20) for the double layer potential ansatz.

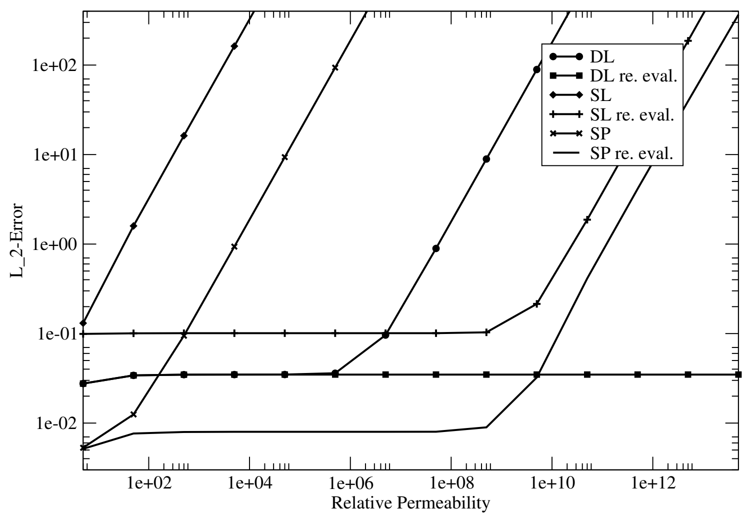

Figure 1: The $L_2(\Gamma)$-error of the gradient plotted versus the relative permeability for all formulations.

Indeed, the error for the single layer potential ansatz and the error for the Steklov–Poincaré operator formulation increase dramatically without the rewritten evaluation for increasing μ_r. The modified evaluation solves that problem for a large range of values of μ_r. However, the rewritten evaluation is only feasible up to a relative permeability of about $5 \cdot 10^9$. For higher permeabilities the error of the evaluation increases. Without taking care of the simply connected domain, the double layer potential approach produces roughly the same accuracy up to a permeability of $5 \cdot 10^6$. For higher permeabilities the accuracy decreases dramatically again. However, the accuracy for the rewritten evaluation (3.20) seems to be stable even up to $\mu_r = 5 \cdot 10^{19}$. Comparing the accuracy of the three methods, the Steklov–Poincaré operator formulation gives better results than the double layer potential formulation which in turn is more accurate than the single layer potential ansatz.

Concluding, the rewritten evaluations produce a higher accuracy for simply connected domains in all our examples. Further on these rewritten evaluations will be used for all three approaches in the case of simply connected domains.

5.2 Ring

As a multi–connected domain, a three–dimensional ring with a square as cross section (Fig. 2) is considered and approximated by several surface meshes. The excitation field is produced by one conductor loop. The radius of the ring is 0.1, and the length and height of the cross–section are 0.05. The radius of the conductor loop is 0.1. The coil current is 500 A.

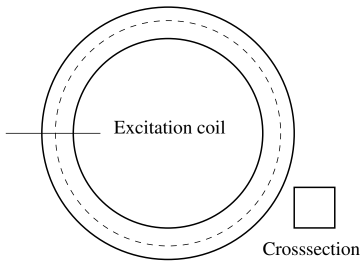

Figure 2: 2D projection of the ring and dotted line of evaluation points.

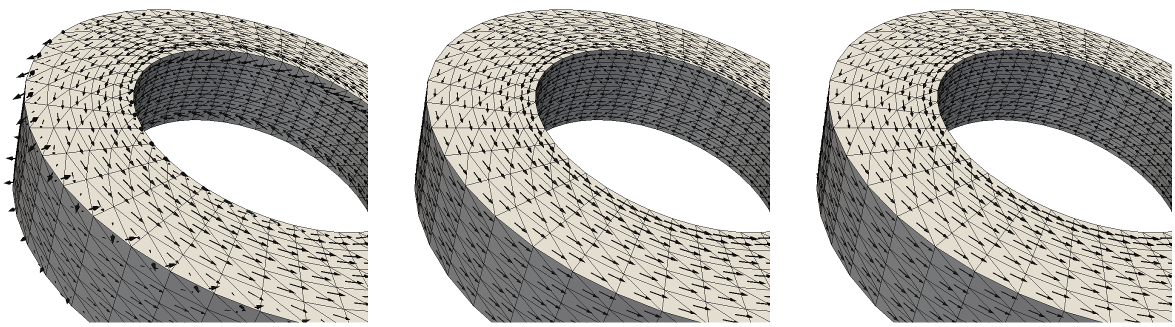

Figure 3: Approximations of $\boldsymbol{H}$ for the single layer potential ansatz (left), the double layer potential ansatz (middle) and for the Steklov–Poincaré operator formulation (right) for $\mu_r = 50000$ and 2024 triangles.

In Fig. 3, the magnetic field $\boldsymbol{H}$ on the interior of the boundary is plotted in the centers of each triangle for the single layer potential ansatz on the left–hand side, the double layer ansatz in the middle and for the Steklov–Poincaré operator formulation on the right–hand side. Further away from the edges the results look alike, whereas towards the edges the vector fields differ significantly. Especially in the last two elements towards the geometrical edges, we observe a non–physical approximation by the single layer potential approach. If we fix such an observation point and refine the mesh further, the magnetic field at that observation point for the single layer potential formulation converges against the result of the Steklov–Poincaré approach and the double layer potential ansatz, which both show good approximations of the magnetic field. It can be concluded that the approximation of the magnetic field towards the geometrical edges for the single layer potential formulation has a very low accuracy. The same effect was observed for all tested μ_r in all examples where edges appear. For meshes, which are graded towards the geometrical edges, the effect is even worse.

Additionally, the magnetic field for a relative permeability $\mu_r = 50000$ is evaluated along the dotted line in the center of the cross section as shown in Fig. 2. It is well known that for $\mu_r \to \infty$ the magnitude of the magnetic field tends towards a uniform distribution along this line. In Fig. 4 and Fig. 5, the magnitudes of the magnetic field are plotted for refinement levels one to five (L1–L5) with 560, 2024, 8096, 32384 and 128832 plane triangular elements.

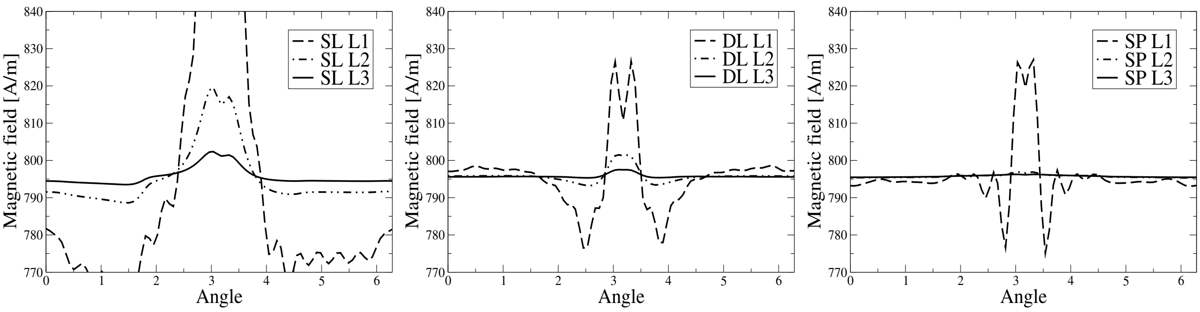

Figure 4: Magnetic field along the dotted line of the ring.

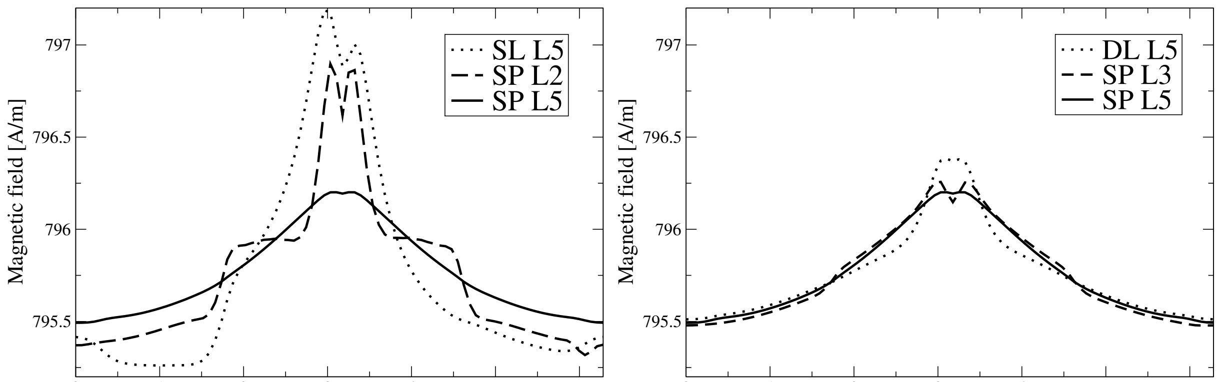

Figure 5: Closeup of the magnetic field along the dotted line of the ring.

For the coarsest mesh the geometrical approximation dominates the errors for all three approaches, however the single layer potential ansatz (SL) is significantly worse than the double layer potential approach (DL) and the Steklov–Poincaré operator formulation (SP). After one refinement, the geometry seems to be dissolved fine enough and one can observe a significant increase in the accuracy especially for the Steklov–Poincaré operator formulation and almost similar but slightly smaller for the double layer potential approach. For the single layer potential ansatz the accuracy is far worse. The second and third level of the Steklov–Poincaré operator formulation do not differ that much in Fig. 4 and the almost uniform distribution is already visible. Taking a closer look at the zooms in Fig. 5, the single layer potential ansatz on level five (SL L5) is comparable with the Steklov–Poincaré operator formulation on level two (SP L2), whereas the double layer potential approach for level five (DL L5) is comparable to the Steklov–Poincaré operator formulation on level three (SP L3).

Furthermore in Table 1, the computational times for the ring are given in seconds.

L	# Elements	SL	DL	SP
1	560	1	5	13
2	2024	5	46	81
3	8096	14	87	268
4	32384	75	448	1443
5	128832	248	1623	4832

Table 1: Solution time for the ring in seconds

The computational times include the setup and solving of the linear systems as well as the evaluation in the interior points and the computation of the gradient on the surface. For a fixed level L, the increase of computational times from the single layer potential ansatz to the double layer potential approach is mainly due to the setup of the additional matrices, the higher polynomial degree of the ansatz and test functions, and the solution of the second system of linear equations. In the case of the Steklov–Poincaré operator formulation, all boundary integral operators have to be computed and local Dirichlet boundary value problems have to be solved in each iteration step of the global system. If we take into account the accuracy of the approaches, the Steklov–Poincaré operator formulation turns out to be comparable with respect to computational times. A comparison is given in Table 2. The solution of the Steklov–Poincaré operator formulation at level five was chosen as a reference solution. In Table 2 the method, the number of elements, the solution time, and the relative error of the point evaluation in the l_2 norm are given for some selected computations.

The error of the single layer potential ansatz at level five is $4.4 \cdot 10^{-4}$. The other two approaches at similar accuracy outperform the single layer potential ansatz by a factor of three. For this accuracy the double layer potential approach and the Steklov–Poincaré operator formulation are almost identical comparing the computational times. However, the accuracy of the Steklov–Poincaré operator formulation is twice as high. Comparing the last level of the double layer potential approach to level three of the Steklov–Poincaré operator formulation, the latter is clearly faster and yields a higher accuracy.

Method	# Elements	Solution Time	rel. l_2-error
DL L3	8096	87	5.25e-4
SL L5	128832	248	4.40e-4
SP L2	2024	81	2.45e-4
DL L5	128832	1623	7.79e-5
SP L3	8096	268	3.24e-5

Table 2: Comparison of the different method for different levels.

Remark 5.1 *The presented computational times depend highly on the implementation of the boundary element method. Our integration routines are based on semi–analytic integration formulae* [21] *and exploit the lowest order elements in K_h' as well as the large blocks of zero entries in K_h and K_h'. The fast multipole method is optimal suited for a low number of matrix times vector multiplications. Therefore our implementation is more favorable for the potential approaches.*

The use of integration routines based on the Duffy transformation [7] *would not give the potential approaches such an advantage. The use of the adaptive cross approximation* [1] *would increase the setup and evaluation times in general, but the times for solving a system would be reduced significantly. The Steklov–Poincaré operator formulation would benefit a lot in comparison to the potential approaches.*

5.3 Controllable reactor

All discussed formulations are finally compared for the computation of the magnetostatic field of a controllable reactor. Controllable reactors, sometimes called shunt reactors, are important components in Extra/Ultra High Voltage power systems used for voltage regulation issues. One of their important roles is to compensate the reactive power. Typically fixed shunt reactors are used for such compensation. Alternative concepts introduced recently are controllable reactors. The controlling effect of an orthogonal flux type controllable reactor is achieved by controlling the saturation level of the parts of the magnetic core (saturable reactor). The key information when analyzing this kind of devices are the controllable reluctances.

Fig. 6 shows the typical structure of a controllable reactor. The cylindric structure in the middle, which is wrapped by the main winding in the complete setup, consists of alternating layers of iron discs and control discs. By adjusting the current in the windings wounded around the control discs the total inductance, i.e., the reluctance of the reactor can be controlled. The simulation of such a reactor model is featured by the most of the requirements as mentioned in the introduction: complex structure, small gaps between fix and controllable discs having a major impact on the cross–talk between the discs, sharp edges of the discs influencing the accuracy of the calculation, treatment of the continuous changes of the saturations with the changes of the DC current in control windings, etc.

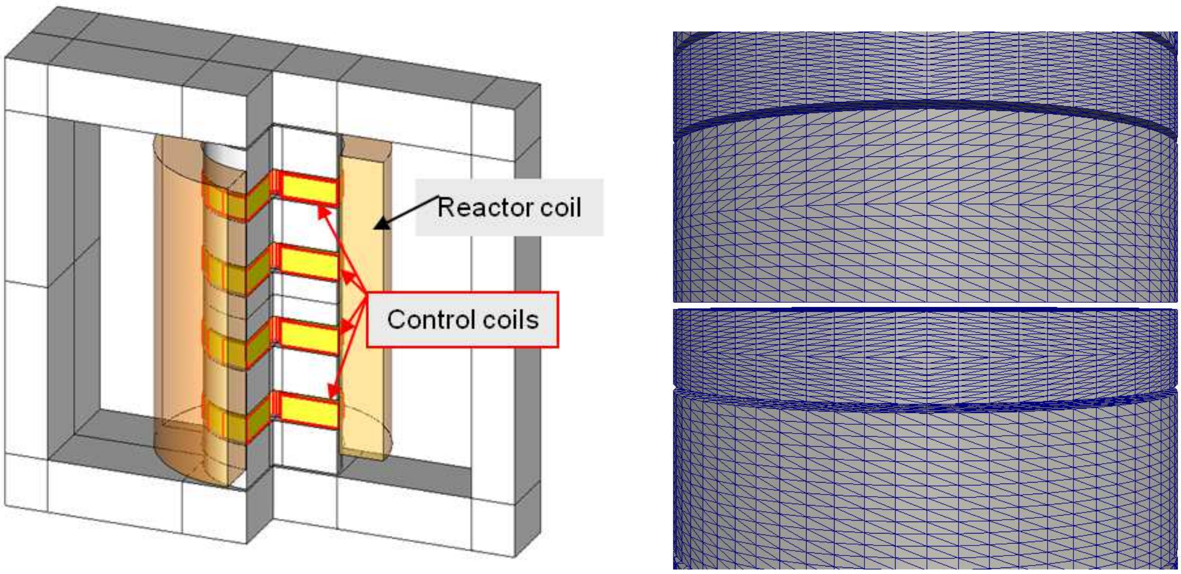

Figure 6: Controllable reactor and a closeup of the small gaps.

For the comparison purpose in this paper we assume a linear and isotropic behavior of the magnetic material with a relative permeability of $\mu_r = 200$. The reactor is meshed with 122880 triangular elements. The results of the three approaches are plotted in Fig. 7. The plots show the magnetic field on the surface of one of the iron discs.

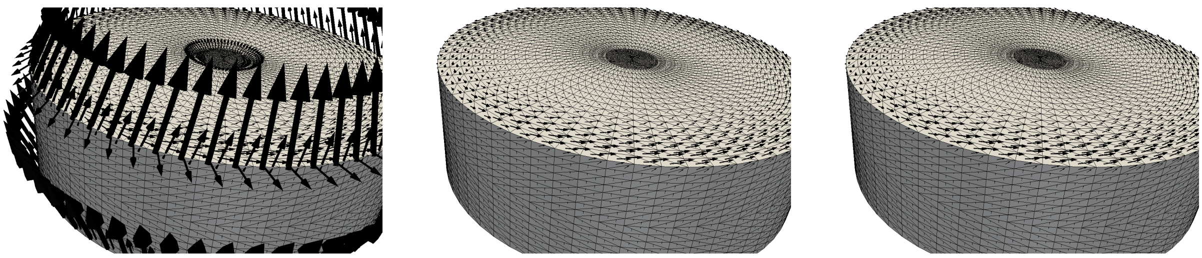

Figure 7: Magnetic field of the single layer potential ansatz (left), the double layer potential ansatz (middle), and the Steklov–Poincaré operator formulation (right) for $\mu_r = 200$.

As expected the same phenomena at corners and edges appears as in the example of the ring as discussed in Sect. 5.2. Essentially the magnetic field near edges is completely different for the single layer potential ansatz. Additionally, the result differs close to the center of the surface of the disc, where the boundary is smooth. This can be explained by the fact, that the gap to the next control disc is very small and these control discs have a small hole in the middle. Thus a corner is very close to these elements, which seems to disrupt the solution on the iron disc.

6 Conclusions

We presented three boundary integral approaches and compared them with respect to accuracy and computational times. In contrast to many other formulations in the literature, all presented formulation are not only applicable to simply connected domains but to multiple connected domains, too. We have proven the equivalence of the single and double layer potential formulations and the Steklov–Poincaré operator formulation for the considered transmission problem on the continuous level. For the discrete systems this is not the case anymore. The single layer potential ansatz, which seems to be the easiest to implement and faster on the first glance, shows really bad approximations towards geometrical edges and in general lower orders of convergence for the considered examples. The double layer potential approach and the Steklov–Poincaré operator formulation provide good approximations close to the edges and significantly higher accuracy. In particular, the Steklov–Poincaré operator formulation gives the best approximations. In our examples the potential approaches needed one to three additional uniform refinements to achieve a comparable accuracy. Requiring a certain accuracy, the Steklov–Poincaré operator formulation and the double layer potential approach are superior to the single layer potential ansatz. For high accuracy, the Steklov–Poincaré operator formulation is the most favorable one. In addition, the Steklov–Poincaré operator formulation is designed to handle settings with several different permeabilities and many subdomains.

Acknowledgement

This work was supported by the FP7 Marie Curie IAPP Project CASOPT (Controlled Component and Assembly Level Optimization of Industrial Devices, www.casopt.com).

References

[1] M. Bebendorf, S. Rjasanow: Adaptive low–rank approximation of collocation matrices. Computing 70 (2003) 1–24.

[2] A. Bossavit: A rationale for edge–elements in 3D fields computations. IEEE Trans. Magn. 24 (1988) 74–79.

[3] A. Buchau, W. M. Rucker, O. Rain, V. Rischmüller, S. Kurz, S. Rjasanow: Comparison between different approaches for fast and efficient 3D BEM computations. IEEE Trans. Magn. 39 (2003) 1107–1110.

[4] M. Costabel, E. P. Stephan: Boundary integral equations for mixed boundary value problems in polygonal domains and Galerkin approximations. In: Mathematical Models and Methods im Mechanics. Banach Centre Publ. 15, PWN, Warschau (1985) 175–251.

[5] J.–L. Coulomb: Finite elements three dimensional magnetic field computation. IEEE Trans. Magn. 17 (1981) 3241–3246.

[6] L. Demkowicz, J. Kurtz, D. Pardo, M. Paszynski, W. Rachowicz, A. Zdunek: Computing with hp–adaptive finite elements. Vol. 2. Frontiers: three–dimensional elliptic and Maxwell problems with applications. Chapman & Hall/CRC, Boca Raton, 2008.

[7] S. Erichsen, S. A. Sauter: Efficient automatic quadrature in 3-D Galerkin BEM. Comput. Methods Appl. Mech. Eng. 157 (1998) 215–224.

[8] H. Forster, T. Schrefl, R. Dittrich, W. Scholz, J. Fidler: Fast boundary methods for magnetostatic interactions in micromagnetics. IEEE Trans. Magn. 39 (2003) 2513–2515.

[9] L. Greengard, V. Rokhlin: A fast algorithm for particle simulations. J. Comput. Phys. 73 (1987) 325–348.

[10] W. Hafla, F. Groh, A. Buchau, W. M. Rucker: Magnetostatic field computations by an integral equation method using a difference field concept and the fast multipole method. Proceedings of the 10th International IGTE Symposium on Numerical Field Calculation in Electrical Engineering, TU Graz, pp. 262–266, 2002.

[11] K. Ishibashi, Z. Andjelic: Nonlinear magnetostatic BEM formulation using one unknown double layer charge, Proceedings of the 14th International IGTE Symposium 2010, Graz, 2010.

[12] B. Krstajic, Z. Andjelic, S. Miloijkovic and S. Babic: Nonlinear 3D magnetostatic field computation by the integral equation method with surface and volume magnetic charges. IEEE Trans. Magn. 28 (1992) 1088–1091.

[13] M. Kuhn, U. Langer, J. Schöberl: Scientific computing tools for 3D magnetic field problems. In: The mathematics of finite elements and applications, X, MAFELAP 1999, pp. 239–258, Elsevier, Oxford, 2000.

[14] D. A. Lindholm: Notes on boundary integral equations for three-dimensional magnetostatics. IEEE Trans. Magn. 16 (1980) 1409–1413.

[15] C. Magele, H. Stogner, K. Preis: Comparison of different finite element formulations for 3D magnetostatic problems. IEEE Trans. Magn. 24 (1988) 31–34.

[16] I. D. Mayergoyz, P. Andrei, M. Dimian: Nonlinear magnetostatic calculations based on fast multipole method. IEEE Trans. Magn. 39 (2003) 1103–1106.

[17] I. D. Mayergoyz, M. V. K. Chari, J. D'Angelo: A new scalar potential formulation for three–dimensional magnetostatic problems. IEEE Trans. Magn. 23 (1987) 3889–3894.

[18] G. Of, O. Steinbach, P. Urthaler, Z. Andjelic: Fast boundary element methods for industrial applications in magnetostatics. In preparation.

[19] G. Of, O. Steinbach, W. L. Wendland: The fast multipole method for the symmetric boundary integral formulation. IMA J. Numer. Anal. 26 (2006) 272–296.

[20] T. von Petersdorff, Ch. Schwab: Wavelet approximations for first kind boundary integral equations on polygons. Numer. Math. 74 (1996) 479–516.

[21] S. Rjasanow, O. Steinbach: The fast solution of boundary integral equations. Springer, New York, 2007.

[22] W. M. Rucker, K. R. Richter: Three–dimensional magnetostatic field calculation using boundary element method. IEEE Trans. Magn. 24 (1988) 23–26.

[23] O. Steinbach: Artificial multilevel boundary element preconditioners. Proc. Appl. Math. Mech. 3 (2003) 539–542.

[24] O. Steinbach: Numerical approximation methods for elliptic boundary value problems, Springer, New York, 2008.

[25] O. Steinbach, W. L. Wendland: The construction of some efficient preconditioners in the boundary element method. Adv. Comput. Math. 9 (1998) 191–216.

[26] O. Steinbach, W. L. Wendland: On C. Neumann's method for second–order elliptic systems in domains with non–smooth boundaries. J. Math. Anal. Appl. 262 (2001) 733–748.

Erschienene Preprints ab Nummer 2006/1

2006/1	S. Engleder, O. Steinbach: Modified Boundary Integral Formulations for the Helmholtz Equation.
2006/2	O. Steinbach (ed.): 2nd Austrian Numerical Analysis Day. Book of Abstracts.
2006/3	B. Muth, G. Of, P. Eberhard, O. Steinbach: Collision Detection for Complicated Polyhedra Using the Fast Multipole Method of Ray Crossing.
2006/4	G. Of, B. Schneider: Numerical Tests for the Recovery of the Gravity Field by Fast Boundary Element Methods.
2006/5	U. Langer, O. Steinbach, W. L. Wendland (eds.): 4th Workshop on Fast Boundary Element Methods in Industrial Applications. Book of Abstracts.
2006/6	O. Steinbach (ed.): Jahresbericht 2005/2006.
2006/7	G. Of: The All–floating BETI Method: Numerical Results.
2006/8	P. Urthaler, G. Of, O. Steinbach: Automatische Positionierung von FEM–Netzen.
2006/9	O. Steinbach: Challenges and Applications of Boundary Element Domain Decomposition Methods.
2006/10	S. Engleder: Stabilisierte Randintegralgleichungen für äussere Randwertprobleme der Helmholtz–Gleichung.
2007/1	M. Windisch: Modifizierte Randintegralgleichungen für elektromagnetische Streuprobleme.
2007/2	M. Kaltenbacher, G. Of, O. Steinbach: Fast Multipole Boundary Element Method for Electrostatic Field Computations.
2007/3	G. Of, A. Schwaigkofler, O. Steinbach: Boundary integral equation methods for inverse problems in electrical engineering.
2007/4	S. Engleder, O. Steinbach: Stabilized Boundary Element Methods for Exterior Helmholtz Problems.
2007/5	O. Steinbach, G. Unger: A Boundary Element Method for the Dirichlet Eigenvalue Problem of the Laplace Operator.
2007/6	O. Steinbach, M. Windisch: Modified combined field integral equations for electromagnetic scattering.
2007/7	S. Gemmrich, N. Nigam, O. Steinbach: Boundary Integral Equations for the Laplace–Beltrami Operator.
2007/8	G. Of: An efficient algebraic multigrid preconditioner for a fast multipole boundary element method.
2007/9	O. Steinbach (ed.): Jahresbericht 2006/2007.
2007/10	U. Langer, O. Steinbach, W. L. Wendland (eds.): 5th Workshop on Fast Boundary Element Methods in Industrial Applications, Book of Abstracts
2008/1	P. Urthaler: Schnelle Auswertung von Volumenpotentialen in der Randelementmethode
2008/2	O. Steinbach (ed.): Workshop on Numerical Simulation of the Maxwell Eqautions. Book of Abstracts.